

Rapid Colorimetric Detection of Sulfite in Red Wine Using Alginate-Copper Laccase Nanozyme with Smartphone as an Optical Readout

Kaayyoo Fikadu Gutema, Membere Leul Mekonnen,* Bitania Teklu Yilma, Tesfaye Eshete Asrat, Jan Dellith, Marco Diegel, Andrea Csáki, and Wolfgang Fritzsche



Cite This: *ACS Meas. Sci. Au* 2025, 5, 145–154



Read Online

ACCESS |

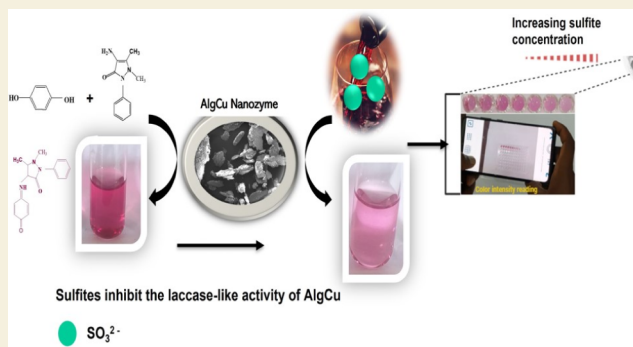
Metrics & More

Article Recommendations

Supporting Information

ABSTRACT: Compared with the conventional analytical methods, nanozyme-based colorimetric sensors offer simpler and more accessible solutions for point-of-need food safety monitoring. Herein, Alginate-Cu (AlgCu) is reported as a robust laccase mimetic nanozyme for the colorimetric detection of sulfite in red wine, a common preservative in winemaking. AlgCu represents a rational design of nanozymes where the multifunctional group alginate is used as a coordination environment for the Cu catalytic center, mimicking the amino acids microenvironment in the natural laccase. The laccase activity of the AlgCu is evaluated using 2,4-dichlorophenol as a model substrate, where its oxidized product reacts with 4-aminoantipyrine, forming a reddish-pink compound with an absorption peak at 510 nm. The result showed that the AlgCu exhibited 32.81% higher laccase activity than pristine copper NPs, highlighting the role of a coordination environment in improving catalytic activity. The addition of sulfite decreased the intensity of the catalytic chromogenic product, confirming that sulfite inhibited the laccase mimetic activity of AlgCu. The observed inhibition is linearly related to the sulfite concentration from 2 to 100 μM ($R^2 = 0.996$), enabling the detection of sulfite down to 0.78 μM . Furthermore, a sulfite concentration down to 4.9 μM could be detected by integrating the colorimetric assay with smartphone color readouts. Analysis of sulfite-spiked red wine samples gave recoveries between 96 and 106%. Overall, the obtained analytical figures of merits signify AlgCu as a robust nanozyme-based colorimetric chemosensor suitable for a point-of-need application in wine quality control and food safety monitoring in general.

KEYWORDS: colorimetric detection, copper–alginate, food safety monitoring, laccase nanozyme, sulfite, wine



1. INTRODUCTION

Sulfites are commonly used in food and beverage production due to their antioxidant and antimicrobial properties.¹ In winemaking, sulfites are widely used to inhibit browning, preserve color over extended shelf periods, and maintain flavor and freshness.¹ However, overconsumption of sulfite exposes humans to various health problems, such as respiratory and cardiovascular diseases. Moreover, it is a cause of asthma and allergic reactions and contributes to lung cancer.² Consequently, the European Union (EU) requires wines to be clearly labeled if they exceed 10 mg/L.³

The conventional analytical method suggested by the Association of Analytical Chemists (AOAC) for sulfite analysis from wine involves Ion chromatography coupled with amperometry detection.^{4,5} However, this method suffers from sensitivity to interference and multistep sample preparations. Other methods are also reported for sulfite analysis, including electrochemical detections,^{6,7} chromatographic (HPLC-IC),^{2,8} and Surface Enhanced Raman spectroscopy (SERS).⁹ Similarly, these methods involve time-consuming sample preparations and instrumental complexity, necessitating high-label

expertise. Given the high public health risk, developing an easy-to-use and reliable analytical method for sulfites is essential, particularly convenient for point-of-need applications.

Enzyme-based colorimetric methods, such as Enzyme-Linked Immunosorbent Assay (ELISA), have been widely used as rapid analysis options in food safety monitoring.^{10,11} However, enzymes often face challenges related to operational stability and high production costs, which limits their utility in developing low-cost quality-control tools.^{12,13} In this regard, there is a growing interest in using nanozymes to address such limitations of natural enzymes in various analytical and biotechnological applications. Nanozymes are nanomaterials with inherent enzyme mimetic activity. They catalyze redox

Received: November 14, 2024

Revised: January 16, 2025

Accepted: January 21, 2025

Published: January 29, 2025



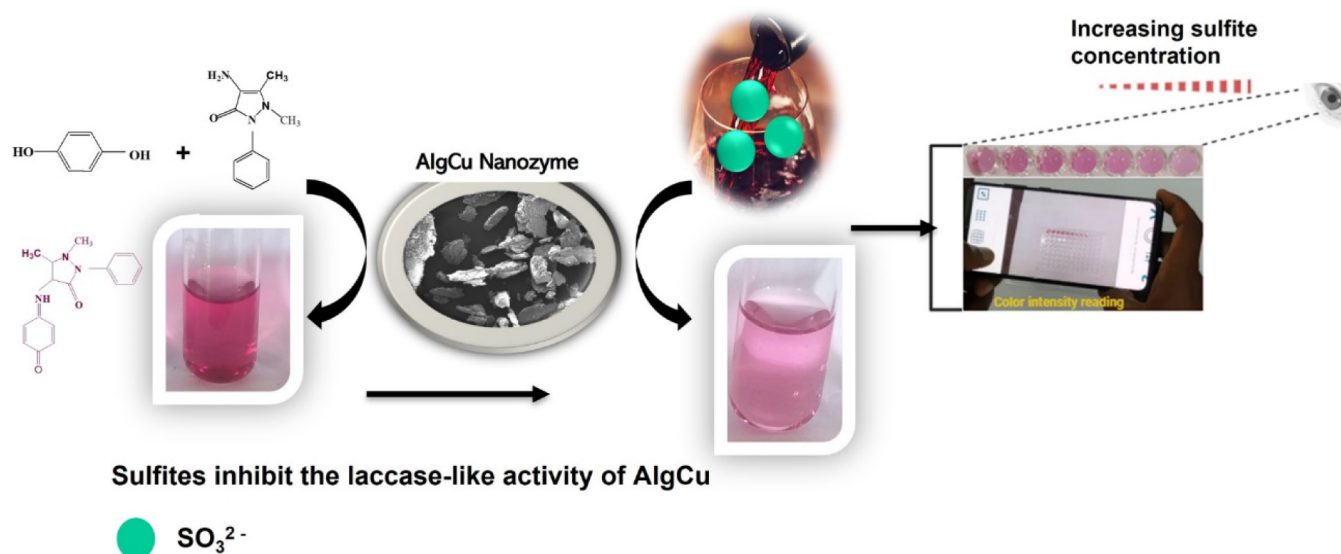


Figure 1. Scheme showing the principle of colorimetric detection of sulfite.

reactions similar to enzymes but with enhanced stability and catalytic efficiency.^{14–16}

Compared to various nanozyme groups, laccase nanozymes are relatively underutilized for analytical applications.^{17–19} Laccase nanozymes represent a multicopper oxidase-based mimetic of the laccase enzyme. These nanozymes can oxidize phenolic compounds, leading to the formation of colored products.^{20–22} This characteristic enables the colorimetric detection of various phenol-containing analytes.^{23,24} While most colorimetric detection methods involving laccase nanozymes focus on the direct colorimetric response of oxidized phenolic compounds, it is also possible to develop colorimetric assays for nonphenolic analytes. This can be achieved by measuring the corresponding color intensity change resulting from their inhibition or enhancement effects on the laccase mimetic activity of the nanozyme.^{25,26}

Various laccase nanozymes are reported for colorimetric detection and degradation of phenol-containing analytes. However, not all of these embrace a rational design approach, which requires a multifunctional group (such as amino, hydroxyl, and carboxylic) in a coordination environment with the copper catalytic active center.^{27–31} Despite this, some encouraging works have already been reported using peptides/nucleotides²² and multifunctional group polymers,^{20,21,32} as a coordination environment for the copper catalytic centers. However, realizing such sensors for real-life sensing applications is still hindered due to the lack of rational design and extensive mechanistic study.

Hence, this study investigates the laccase mimetic activity of alginate copper (AlgCu) for the colorimetric detection of sulfite from red wine. The choice of AlgCu represents a rational design of laccase nanozyme where the catalytic active center (copper) is coordinated with the functional sites of the polymer.^{33,34} The hydroxyl/carboxylic group in the polymer can act as electron transfer channels, enhancing the catalytic activity similar to the amino acid microenvironment in the laccase enzyme. Moreover, AlgCu provides a more robust and cost-effective nanozyme-based sensor than the usual nucleotide/amino acid-based nanozymes. The laccase-like catalytic activity of AlgCu was investigated using 2,4-dichlorophenol (2,4-DP) as a model phenolic substrate and 4-aminoantipyrine

(4-AP) as a chromogenic substrate. Sulfite inhibited this laccase activity, decreasing the color intensity and forming the basis for the reported colorimetric detection, as illustrated in the scheme in Figure 1.

2. EXPERIMENTAL SECTION

2.1. Materials

All chemicals and reagents used in this research were of analytical grade. 2,4-dichlorophenol (2,4-DP) ($\text{C}_6\text{H}_4\text{Cl}_2\text{O}$, 99%), 4-aminoantipyrine (4-AP) ($\text{C}_{11}\text{H}_{13}\text{N}_3\text{O}$, 99%) hydrochloric (HCl, 37%), and sodium alginate ($\text{NaC}_6\text{H}_7\text{O}_6$, 91%), boric acid (H_3BO_3 , 99.5%), monopotassium phosphate ($\text{KH}_2\text{PO}_4 \cdot \text{H}_2\text{O}$, 97%), and dipotassium phosphate (K_2HPO_4 , 99%), sodium sulfite (Na_2SO_3 , 97%), sodium phosphate dibasic ($\text{Na}_2\text{HPO}_4 \cdot 12\text{H}_2\text{O}$, 99%), copper sulfate pentahydrate (CuCl_2 , 99%), and Tris buffer ($\text{C}_4\text{H}_{11}\text{NO}_3$, 99%), were purchased from Sigma-Aldrich, USA. Sodium hydroxide (NaOH, 99%), sodium chloride (NaCl, 99%), potassium chloride (KCl, 99%), ethanol ($\text{C}_2\text{H}_5\text{OH}$, 99%), acetic acid (CH_3COOH , 37%) and sodium acetate ($\text{C}_2\text{H}_3\text{NaO}_2$, 99%) were supplied by Central Drug House, India. Red Wine samples were bought from a local grocery in Addis Ababa, Ethiopia.

2.2. Synthesis of the Nanozyme

Alginate-copper nanozyme synthesis is based on a modified protocol from a previous report.³⁵ Briefly, 0.15 g of sodium alginate was added to 10 mL of distilled water and stirred at room temperature until dissolved completely. Then, 10 mL of 0.03 M copper sulfate was added, followed by 5 mL of 0.5 M NaOH. The resulting mixtures were stirred for 2 h at 60 °C. Finally, the product was washed twice with distilled water and ethanol, centrifuged each time, and vacuum oven-dried at 40 °C overnight.

2.3. Characterization of the Nanozyme

All parameter optimizations, kinetics, and absorption measurements were done using a UV–vis spectrophotometer (JASCO V770, Japan). A scanning electron microscope (SEM, JSM-6700F; JEOL Ltd., Japan) was used to study the morphology of the synthesized AlgCu nanozyme. The energy dispersive X-ray elemental mappings (EDX) were performed using a silicon

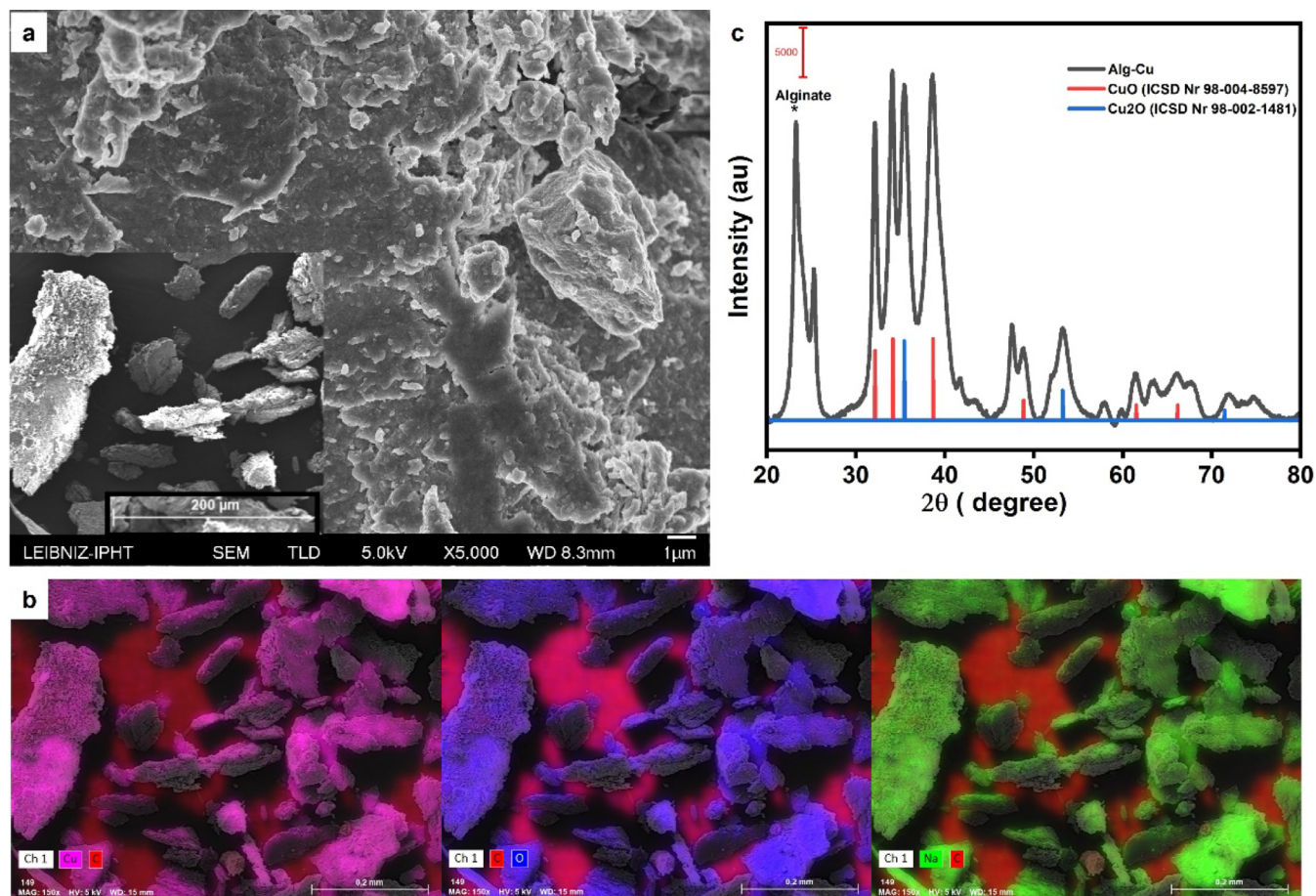


Figure 2. (a) SEM image; (b) X-ray elemental mapping; (c) XRD pattern of AlgCu.

drift detector (SDD; XFlash7100; BRUKER Nano GmbH, Berlin, Germany). An X-ray diffraction spectrophotometer (XRD) (X'Pert PRO MPD-DY32S; Malvern Panalytical, Netherlands) was utilized to investigate the phase composition and crystal structure of the nanozyme. Fourier Transform Infrared spectrophotometer (FTIR) (Thermo Scientific Nicolet Evolution-300, USA) was applied to investigate the functional groups in synthesized nanozyme. The chemical state and surface composition of AlgCu were analyzed using an X-ray photoelectron spectrophotometer (XPS) (AXIS Supra⁺ Kratos Analytical, UK).

2.4. Laccase-like Activity

The preliminary laccase-like activity of the synthesized nanozyme was examined using 2,4-DP as a model phenolic substrate and 4-AP as a chromogenic agent in Tris buffer (pH 7). In a typical assay, 100 μL 4-AP aqueous solution (1 mg/mL) and 100 μL 2,4-DP aqueous solution (1 mg/mL) were mixed in 700 μL Tris buffer (0.1 M, pH 7). After that, 100 μL of 2 mg/mL nanozyme was added to the above mixture. The reaction mixture was incubated at different times, and the absorbance of the colored product was measured using a UV-vis spectrophotometer. The effect of precursor ratio, the amount of nanozyme, reaction time, pH, and type of buffer species was studied by varying one factor at a time. The steady-state kinetics of the synthesized AlgCu nanozyme was examined by varying the concentration of 2,4-DP. For each of these reactions, the concentration of 4-AP was in excess. The absorbance of the resulting colored product was measured

at a fixed wavelength (510 nm) using a time course measurement. The kinetic parameters K_m and v_{\max} were calculated from the Lineweaver–Burk plot (eq 1), which is the double reciprocal plot of the Michaelis–Menten (eq 2).

$$\frac{1}{v} = \frac{K_m}{v_{\max}} \frac{1}{[S]} + \frac{1}{v_{\max}} \quad (1)$$

$$v = \frac{v_{\max}}{K_m + [S]} \quad (2)$$

Where v is the initial velocity, v_{\max} is the maximum velocity of the reaction, $[S]$ is the initial concentration of the substrate, and K_m is the Michaelis constant, which indicates the enzyme's affinity for the substrate.³⁶

2.5. Colorimetric Detection of Sulfite

Colorimetric detection of sulfite was conducted as follows. Different concentrations of Sodium sulfite standard solution (0–100 μM) in Tris buffer (0.1 M, pH 7) were mixed with the reaction mixture containing 2,4-DP (1 mg/mL, 100 μL), 4-AP (1 mg/mL, 100 μL) and AlgCu nanozyme (2 mg/mL, 100 μL). The reaction was kept for 30 min, and the absorbance of the resulting colored solution was measured at 510 nm. A calibration curve showing the relationship between the concentration of sulfite and absorbance (ΔA vs C) was plotted, from which the analytical figures of merits were calculated according to the International Conference on Harmonization (ICH).³⁷ The application of the sensor for point-of-need application in food safety monitoring was demonstrated using a Spotxcel Reader 1.1 installed on a

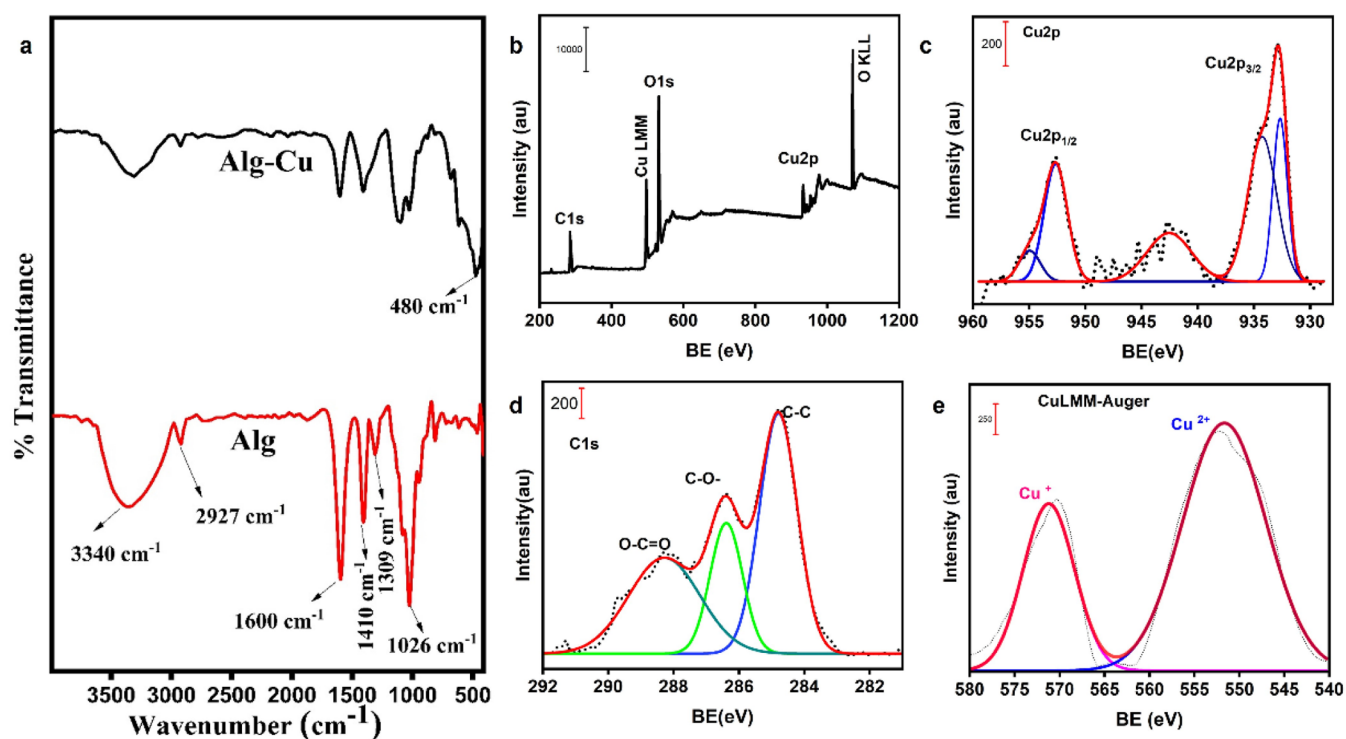


Figure 3. (a) FTIR spectrum; (b) wide scan XPS spectrum; high-resolution spectrum (c) Cu 2p, (d) C 1s, and (e) Auger Cu LMM of AlgCu nanozyme.

smartphone as a color (optical) readout. All data were statistically analyzed using Origin Pro 2024b software.

2.5.1. Detection of Sulfite in the Wine Sample. Known concentrations of sulfite standard were spiked into wine samples brought from the grocery store and thoroughly mixed with a shaker. After centrifugation, the supernatant was filtered with a 0.45 μm PVDF membrane, and the filtrate was analyzed with a similar protocol as in the standard solution. Unspiked samples were also run in parallel. The % recovery of sulfite was calculated using eq 3.

$$\%R = \frac{C_{\text{spiked}} - C_{\text{unspiked}}}{C_{\text{added}}} \times 100 \quad (3)$$

C_{spiked} and C_{unspiked} are the concentrations found in sulfite spiked and unspiked wine samples, and C_{added} is the actual concentration of sulfite added to the wine sample.

3. RESULTS AND DISCUSSION

3.1. Synthesis and Characterization of AlgCu

AlgCu nanozyme was synthesized by *in situ* reduction of Cu^{2+} in an aqueous solution of sodium alginate. As shown in Figure S1a, the reaction product appeared as a brown, less viscous gel, indicating the formation of a cross-linked gel, a characteristic of alginate with divalent ions.³⁸ The SEM images (Figure 2a) show the flake of AlgCu where copper nanoparticles are dispersed in the polymeric matrix. The EDX elemental map and spectrum (Figures 2b and S1b) also show the uniform distribution of main elements such as C, O, and Cu. As seen in the XRD pattern (Figure 2c), the peaks at 2θ of 35.48°, 53.25°, and 71.82° belong to diffractions from (111), (020), and (311) Cu_2O phases, respectively (ICSD No 98-002-1481). The peaks at 2θ of 34.04°, 38.06°, 48.97°, 61.16°, and 66.05° represent diffraction from (002), (111), (202), (113), and

(311) planes of monoclinic CuO (ICSD No 98-004-8597). The crystallite size was calculated using Debye–Scherrer’s equation (eq 4) was 6.97 nm.

$$d = \frac{k\lambda}{\beta \cos \theta} \quad (4)$$

Where k is the Debye–Scherrer constant (0.89), λ is the X-ray wavelength (Cu- $K_{\alpha 1}$ radiation, 0.1546 nm), β is the full-width at half-maximum of the XRD line in radians, and θ is the half diffraction angle.

Further, FT-IR investigation (Figure 3a) of functional groups in the polymer revealed characteristic bands at 3340, 1600, and 1026 cm^{-1} representing the stretching vibration of $-\text{OH}$, Carbonyl, and $\text{C}-\text{O}-\text{C}$, respectively. However, after the composite formation, the intensity of these bands was reduced, and additional new bands at 480 cm^{-1} appeared, indicating the coordination of the metal with the hydroxyl/carboxylic groups. This is also consistent with the observations made in previous reports.^{39–41} XPS was used to study the chemical states of AlgCu. The wide-scan XPS spectrum (Figure 2b) confirms the presence of Cu, O, and C elements in the nanozyme, with Cu accounting for 24.0% of the atomic composition. Deconvolution of the high-resolution spectra of Cu 2p (Figure 3c) revealed peaks at 934.57 and 954.25 eV, corresponding to the Cu 2p_{3/2} and Cu 2p_{1/2} electrons of the Cu(II). Meanwhile, the peaks at the lower BE and 932.75 and 952.54 represent the Cu 2p_{3/2} and Cu 2p_{1/2} electrons of the Cu(I) oxidation state. The satellite peaks at 942.04 eV, corroborating the Cu(II) state. The deconvolution of the C 1s spectrum (Figure 3d) also shows three peaks at 284.79, 286.39, and 288.28 eV corresponding to C–C, C–O– and $-\text{O}-\text{C}=\text{O}$ bonds, respectively. Further, the deconvolution of the Auger Cu LMM peak (Figure 3e) revealed peaks at 551.67 and 571.19 eV, which can be related to Cu(II) and Cu(I),

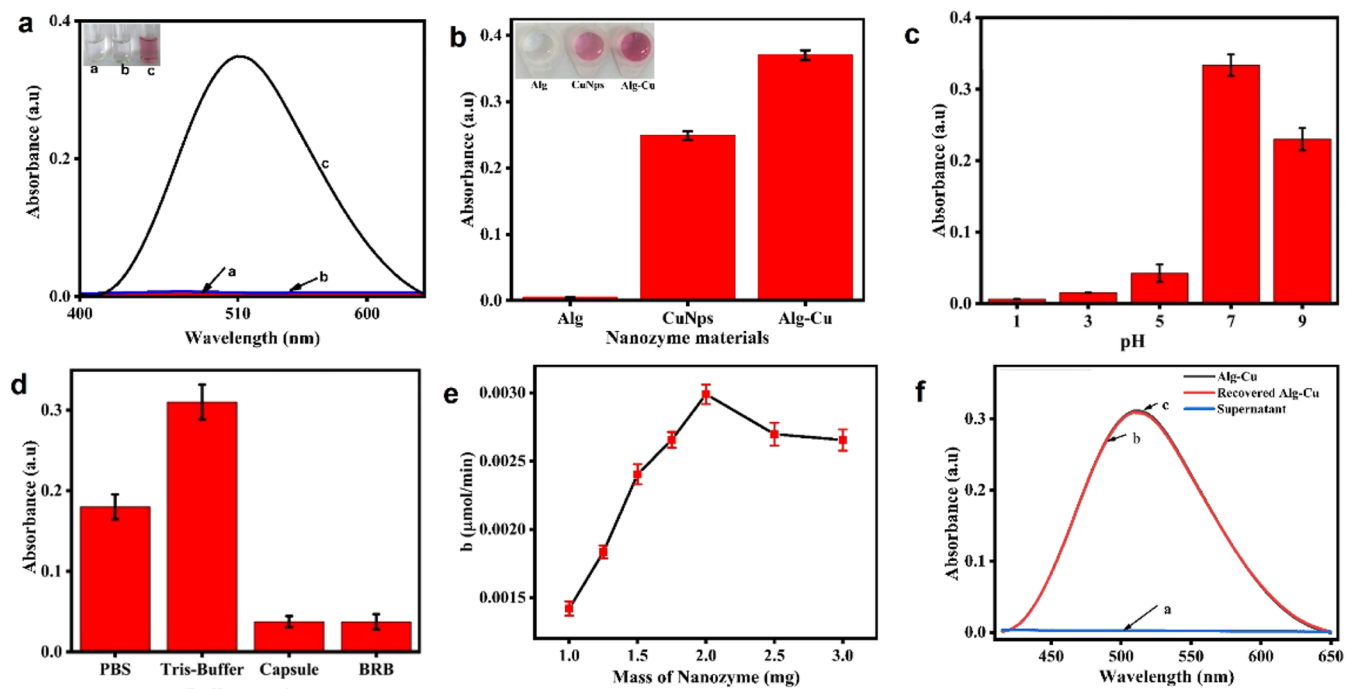


Figure 4. (a) Laccase mimetic activity of AlgCu (a: 2,4-DP + 4-AP in a buffer; b: DP in a buffer; c: AlgCu + 4-AP + 2,4-DP); (b) comparison of laccase activity; effect of (c) pH, (d) buffer species, and (e) amount of nanozyme; (f) laccase activity of pristine and recovered AlgCu.

respectively. The ratio of Cu(II) to Cu(I) was calculated to be 2.39. This is desirable from the application point of view as the natural laccase is a multicopper oxidase enzyme.

3.2. Laccase-like Catalytic Activity of AlgCu Nanozyme

The laccase-like catalytic activity of AlgCu was evaluated using 2,4-dichlorophenol (2,4-DP) as a model phenolic substrate and 4-aminoantipyrine (4-AP) as a chromogenic agent in Tris buffer (pH 7). As shown in Figure 4a, the addition of AlgCu to the 2,4-DP, 4-AP reaction system led to the formation of a reddish-pink color (inset photo c), which absorbs at 510 nm, indicating the oxidation of 2,4-DP.⁴² Additionally, parallel control experiments were carried out to further validate the role of each component in the reaction. Accordingly, 2,4-DP and 4-AP alone could not produce the expected chromogenic product, corroborating the catalytic role of AlgCu.

Laccase is a group of oxidase enzymes that reduces oxygen to water without producing H₂O₂, making it a green catalyst.⁴³ Hence, this was proved by adding the peroxidase substrate TMB to the reaction mixture. It was expected that if H₂O₂ was produced, as it is in normal peroxidase-catalyzed reactions, the produced H₂O₂ would oxidize TMB, resulting in the characteristic blue color (absorption maxima 652 nm).^{44,45} However, as shown in Figure S2, no blue color was observed, confirming the absence of H₂O₂ product. Hence, the AlgCu only showed laccase-like activity. As observed in Figure 4b, alginate alone has no laccase-like activity. However, it enhanced the pristine copper NPs catalytic activity by 32.81%. This increment can be ascribed to alginate hydroxyl and carboxyl groups, which apparently bind to the copper active centers, enhancing the electron transfer similar to the amino acids in the natural laccase enzyme.^{21,46}

The pH of the reaction plays a crucial role as reaction media to facilitate specific enzymatic reactions. Hence, the effect of pH on the laccase-like activity of AlgCu was optimized using various buffer solutions. As shown in Figure 4c, the AlgCu

nanozyme showed a wider working pH with optimum activity at pH 7. The optimal activity of AlgCu at neutral pH can be attributed to the fact that the copper reactive center remains intact at neutral pH. Further lowering of pH may lead to the dissolution of metal ions from the nanozyme. In contrast, more alkaline conditions will result in the binding of hydroxide ions, hence causing its inactivation.⁴⁷ Further, different buffer components, all of which had pH 7, were used to study the effect of buffer species on the catalytic activity. As shown in Figure 4d, AlgCu demonstrated the highest activity in the Tris buffer. The catalytic activity difference could be due to the electrostatic interaction among the buffer species and nanozyme. Tris buffer is positively charged at pH 7 and the electrostatic repulsion between AlgCu and Tris buffer could increase the binding of 2,4-DP with the nanozyme.⁴⁸

As seen in Figure 4e, the optimum activity was obtained at 2 mg/L of the nanozyme. The unit activity calculated based on eq 5 was 0.0016 U/mg. Furthermore, the study investigated whether the catalytic activity originated from potentially leached copper ions or the intact AlgCu. This was done by comparing the activity of the original nanozyme with that of the leached solution. The leached solution was obtained by centrifuging the nanozyme solution, and the supernatant was taken. As shown in Figure 4f, the supernatant did not show laccase activity, whereas the recovered and the original AlgCu exhibited comparable laccase activity. This confirmed that any laccase activity of the nanozyme is from the intact AlgCu structure.

$$b_{\text{nanozyme}} = \frac{V}{\epsilon l} \times \frac{\Delta A}{\Delta t} \quad (5)$$

Where b – the unit activity of the nanozyme, V – volume, ϵ – absorptivity coefficient, l – path length, A – absorbance, and t – time.

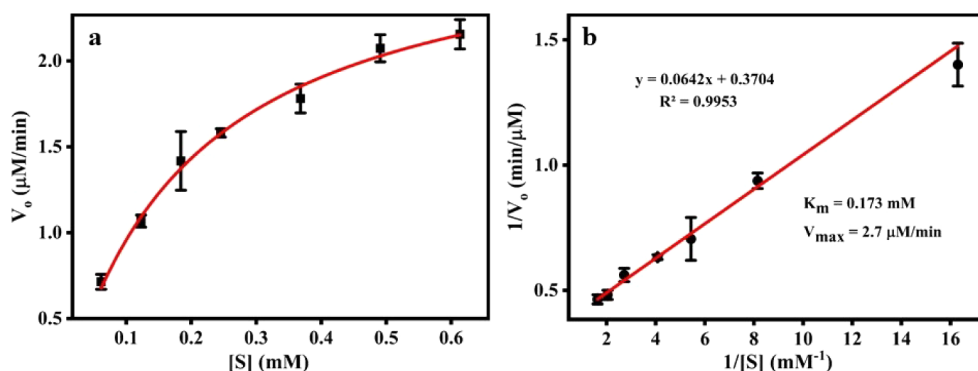


Figure 5. (a) Michaelis–Menten curve; (b) Lineweaver–Burk plots of the AlgCu catalyzed reaction.

3.3. Steady-State Nanozyme Kinetics

The steady-state reaction kinetic was investigated at various concentrations of 2,4-DP as a substrate and a fixed dose of AlgCu. As seen in Figure 5a, the rate of oxidation reaction increased with substrate concentration and followed the typical Michaelis–Menten curve. Accordingly, kinetic parameters were calculated from the Lineweaver–Burk plot (Figure 5b), which is the double reciprocal of the Michaelis–Menten equation. The calculated K_m and v_{max} were 0.173 mM and 2.7 $\mu\text{M min}^{-1}$, respectively (Table 1). Lower K_m often indicates

Table 1. Summary of Kinetic Results from AlgCu Catalyzed Reaction

Substrate	K_m	v_{max}	$^aK_{cat}$
2,4-DP	0.173 mM	2.7 $\mu\text{M min}^{-1}$	$3.6 \times 10^{-4} \text{ min}^{-1}$

$^aK_{cat} = v_{max}/C$, for approximation, only the copper concentration from the XPS result is taken.

better substrate-enzyme interaction. The obtained K_m value for the studied nanozyme is lower than recently reported nanozymes and even much lower than the laccase enzyme (Table S1).⁴⁹ This improved catalytic activity could be ascribed to the presence of a polymer matrix, which provides a coordination microenvironment for improved electron transfer and better access to the substrate.^{45,46}

3.4. Stability and Recyclability of AlgCu Nanozyme

The stability and recyclability of nanozymes play a crucial role in maintaining practical applications of nanozyme.⁵⁰ Hence, the thermal stability of the AlgCu was studied by varying the reaction temperature in a water bath. As seen from Figure 6a,

the activity of the nanozyme increased with temperature until 55 °C, which is followed by a gradual decrease. It is also worth noting that the nanozyme retains 34.6% of its activity even at 95 °C, indicating a robust performance compared to natural laccase, which often loses its activity beyond 40 °C.⁴³ Further, the AlgCu nanozyme retained 70.3% of its activity after 30 days (Figure 6b), indicating improved long time stability. In addition, as seen in Figure 6c, the AlgCu nanozyme retained over a third of its initial activity after the fifth cycle, supporting the sustainable utilization of materials.⁵¹

3.5. Colorimetric Detection of Sulfite

Sulfites, commonly used as preservatives in food and beverages, could have adverse health effects and require careful regulation. Sulfites are added to wine in different forms, including sodium sulfite (Na_2SO_3), sodium bisulfite (NaHSO_3), and potassium metabisulfite ($\text{K}_2\text{S}_2\text{O}_5$), among others. Depending on the conditions, such as pH, these additives are often found to be bound or free. However, due to the acidic nature of wine, free sulfites are the prevalent species, and these forms of sulfites cause different health problems, including hypersensitivity.^{52–54} As a result, we studied these species to demonstrate the capability of nanozyme-based colorimetric sensors as a convenient quality control solution in wine. The effect of sulfite on the catalytic reaction was studied to establish its colorimetric relationship to be used for detection. As seen in Figure 7a, the presence of sulfite slowed the catalytic response, suggesting that sulfite inhibits the laccase-like activity of AlgCu. This could be attributed to the competition of sulfites for binding with the substrate.⁵⁵ Further, the inhibition effect is concentration-dependent, with the intensity of the catalytic chromogenic product

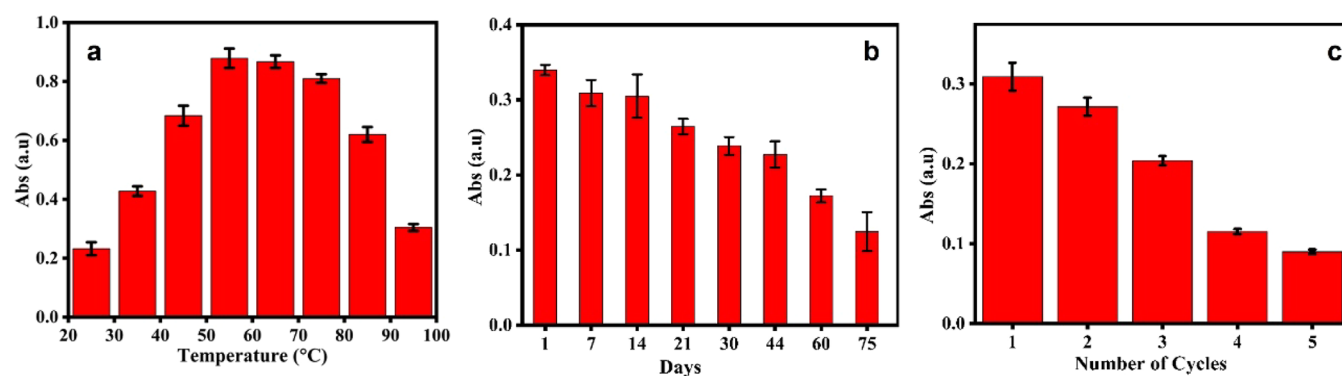


Figure 6. (a) Thermal stability; (b) temporal stability; and (c) recyclability of AlgCu nanozyme.

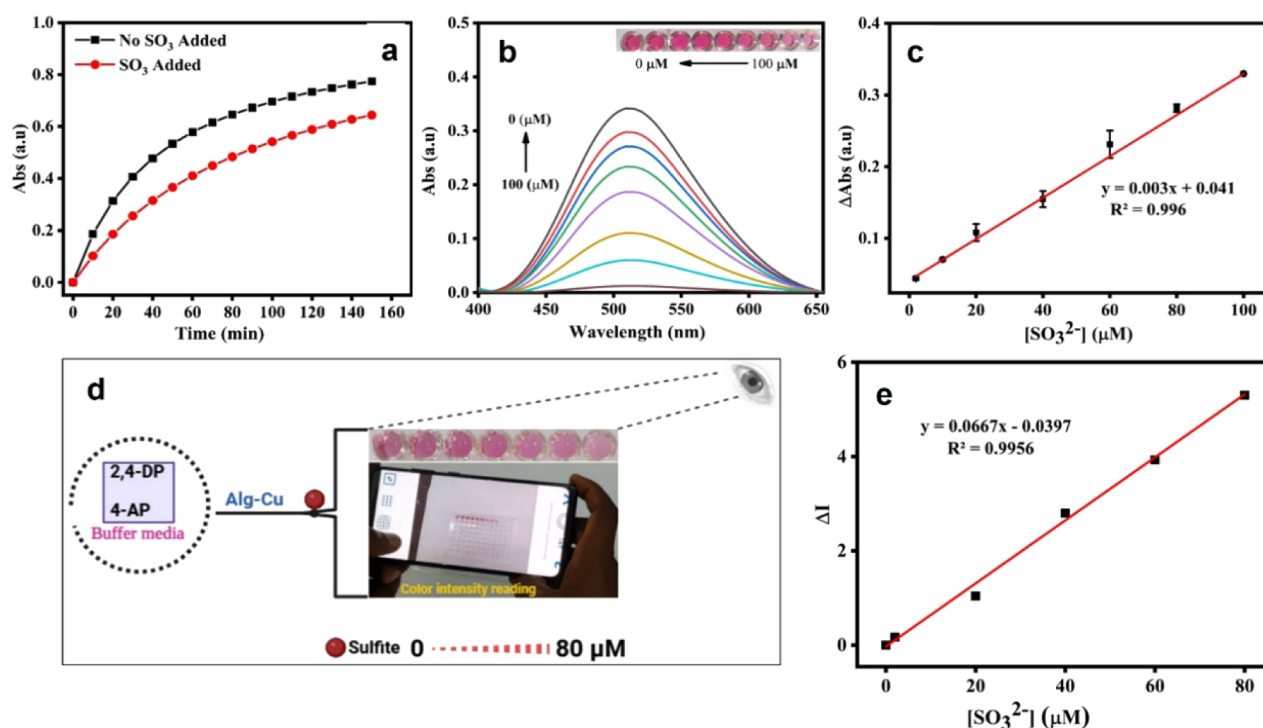


Figure 7. (a) Inhibition effect of sulfite on the laccase activity of AlgCu; (b) absorption spectra of the chromogenic catalytic product in the presence of different concentrations of sulfite; (c) calibration curve for the sulfite detection (ΔA vs C); (d) scheme for smartphone-based sulfite detection; (e) calibration curve obtained from the digital images using the smartphone-based application.

decreasing as the sulfite concentration increased (Figure 7b). Accordingly, the change in color intensity exhibited a linear relationship with the sulfite concentration (ΔA vs C) in the concentration range 2–100 μM ($R^2 = 0.996$) (Figure 7c). Hence, the detection limit (LOD) calculated from the calibration curve as $3.3 \times S_E/m$ is 0.78 μM , where S_E is the response error and m is the slope.⁵⁶ This indicates that the developed colorimetric sensor can detect sulfite well below 10 mg/L, the permissible limit set by standard regulatory bodies.³

3.5.1. Smartphone-Based Colorimetric Sensing of Sulfite. Nanozyme-enabled colorimetric sensors have the potential to be integrated with smartphone-based color readouts, opening up possibilities for point-of-need food safety monitoring applications. Figure 7d shows digital images of the sulfite-inhibited laccase-catalyzed chromogenic product captured using a smartphone. These images were then analyzed using the Spotxel Reader 1.1 color readout application installed on the smartphone. As demonstrated in Figure 7e, the change in color intensity exhibited a linear relationship with the sulfite concentration, enabling the detection of sulfite down to 4.9 μM . This underscores the ease with which the developed nanozyme can be integrated with simple color readout devices, facilitating rapid analytical decision-making in the beverage industry.

3.5.2. Detection of Sulfite in Red Wine. The accuracy of the developed laccase nanozyme for sulfite detection in real samples is studied by analyzing sulfite-spiked red wine. Different sulfite concentrations were spiked to red wine samples following sample pretreatment, as detailed in section 2.6. The colorimetric detection is then carried out using a protocol similar to the standard sulfite detection in the above sections. As seen in Table 2, the average recovery for sulfite ranged from 96 to 106%, which is within the conventional analytical method validation range (80 to 120%).⁵⁷ This

Table 2. Spike-Recovery Results of SO₃²⁻ in Red Wine

SO ₃ ²⁻ added (μM)	SO ₃ ²⁻ found (μM)	Recovery (%)	RSD (%) ($n = 3$)
2.00	2.10	105	2.38
10.00	10.06	106	3.03
40.00	38.4	96	4.12

indicates the suitability of the developed colorimetric sensor for accurate sulfite detection in red wine.

3.5.3. Interference Test. The performance of the developed colorimetric sensor in the presence of potential interferents was also analyzed by adding different interferents that could be present in beverages. Accordingly, the selectivity of the AlgCu nanozyme-based colorimetric sensor was tested using different anions and cations. The inhibition effect was tested separately and with a mixture of all interferents altogether. The concentration of all interferences was 10 folds of the analyte of interest. As shown in Figure 8, the inhibition effect of sulfite on AlgCu activity was 50% higher than that of other interferents, including their mixture. The observed sulfite inhibition effect confirms the selectivity of the developed sensor. The reason could be ascribed to the better binding ability of sulfite anions with the copper center.

3.5.4. Comparison with Other Detection Methods. Compared with the conventional spectrometric-chromatographic methods, nanozyme-enabled colorimetric sensors offer operational simplicity and potential for point-of-need application. Table 3 provides a comparison of the sulfite detection performance of different methods. The table shows that AlgCu laccase nanozyme offered comparable or even a lower detection limit when compared to other reported detection methods. Given its rational design and robustness, with the obtained sensitivity, the developed nanozyme could

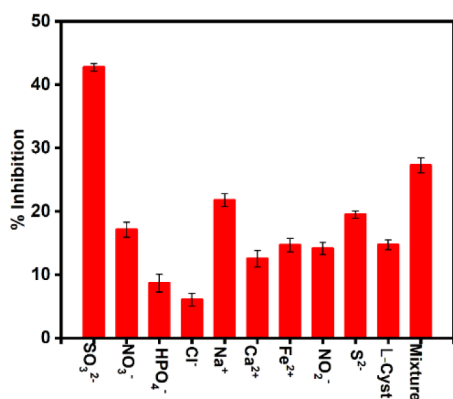


Figure 8. Selectivity of nanozyme in the presence of potential interferents (mixture represents a mixture of all interferences).

Table 3. Comparison of AlgCu Laccase Nanozyme Sensor with Other Methods

Sensor	Method	LOD (μM)	Ref.
LuHCF/poly(taurine)- GCE	Electrochemical	1.33	58
PEGDA-AuNPs	SERS	3.17	9
Bislevulinyl-containing probe	Fluorescence	10	59
MCC-TI Probe	Fluorescence	0.42	60
Phenanthrene imidazole probe	Fluorescence	0.57	61
Co(II)-phthalocyanine complex	Potentiometric	1	62
Co–Mo oxide Peroxidase nanozyme	Colorimetric	0.09	63
MIL-53(Fe/Mn) Peroxidase nanozyme	Colorimetric	0.4	64
Ag ₂ O Peroxidase nanozyme	Colorimetric	10	65
AlgCu Laccase nanozyme	Colorimetric	0.78	This work

bring great potential for point-of-need application for food safety monitoring.

4. CONCLUSION

A robust AlgCu laccase nanozyme was successfully developed for the rapid colorimetric detection of sulfite, a common preservative in winemaking. Morphological and structural analysis shows the presence of multioxidation state copper dispersed on the polymeric matrix. The choice of alginate as a ligand represents a rational design of laccase nanozyme where the catalytic copper centers are coordinated with the OH/COO- functional groups. This improved the catalytic activity of pristine copper by 32.81%, which could be due to the improved electron transfer through a multifunctional group polymeric matrix, similar to the hist-cystine pathway in the natural laccase. A laccase nanozyme-enabled colorimetric detection of sulfite was successfully demonstrated using a smartphone as a color readout. Sulfite showed concentration-dependent inhibition of the laccase mimetic activity of AlgCu, establishing a colorimetric detection down to 0.78 μM . The result suggests the potential of the developed colorimetric sensor for rapid sulfite detection in wine.

■ ASSOCIATED CONTENT

Data Availability Statement

The data supporting this study's findings are available on request from the corresponding author.

SI Supporting Information

The Supporting Information is available free of charge at <https://pubs.acs.org/doi/10.1021/acsmesuresciau.4c00085>.

(a) Digital photo of AlgCu and (b) EDX spectrum of AlgCu nanozyme (Figure S1); AlgCu catalyzed reaction in the presence of TMB (Figure S2); comparison of kinetic parameters of this work with recent reports (Table S1) (PDF)

■ AUTHOR INFORMATION

Corresponding Author

Menbere Leul Mekonnen – Industrial Chemistry Department, Addis Ababa Science and Technology University, Addis Ababa 1647, Ethiopia; Nanotechnology Center of Excellence, Addis Ababa Science and Technology University, Addis Ababa 1647, Ethiopia; orcid.org/0000-0001-9617-853X; Email: menbere.leul@aastu.edu.et

Authors

Kaayyoo Fikadu Gutema – Industrial Chemistry Department, Addis Ababa Science and Technology University, Addis Ababa 1647, Ethiopia

Bitania Teklu Yilma – Industrial Chemistry Department, Addis Ababa Science and Technology University, Addis Ababa 1647, Ethiopia

Tesfaye Eshete Asrat – Industrial Chemistry Department, Addis Ababa Science and Technology University, Addis Ababa 1647, Ethiopia; Nanotechnology Center of Excellence, Addis Ababa Science and Technology University, Addis Ababa 1647, Ethiopia

Jan Dellith – Competence Center for Micro- and Nanotechnologies, Microstructure Analysis Group, Leibniz Institute of Photonic Technology (Leibniz-IPHT), Jena 07745, Germany

Marco Diegel – Competence Center for Micro- and Nanotechnologies, Microstructure Analysis Group, Leibniz Institute of Photonic Technology (Leibniz-IPHT), Jena 07745, Germany

Andrea Csáki – Nanobiophotonics Department, Leibniz Institute of Photonic Technology (Leibniz-IPHT), Jena 07745, Germany

Wolfgang Fritzsche – Nanobiophotonics Department, Leibniz Institute of Photonic Technology (Leibniz-IPHT), Jena 07745, Germany

Complete contact information is available at:

<https://pubs.acs.org/doi/10.1021/acsmesuresciau.4c00085>

Author Contributions

CRedit: **Kaayyoo Fikadu Gutema** data curation, formal analysis, investigation, software, writing - original draft; **Menbere Leul Mekonnen** conceptualization, data curation, formal analysis, funding acquisition, investigation, methodology, project administration, supervision, visualization, writing - original draft; **Bitania Teklu Yilma** data curation, investigation, software; **Tesfaye Eshete Asrat** project administration, supervision, writing - review & editing; **Jan Dellith** formal analysis, investigation, writing - review & editing; **Marco Diegel** formal analysis, investigation, writing - review & editing; **Andrea Csaki** resources, validation, writing - review & editing; **Wolfgang Fritzsche** resources, validation, writing - review & editing.

Notes

The authors declare no competing financial interest.

ACKNOWLEDGMENTS

This work was supported by Addis Ababa Science and Technology University, Nanotechnology Center of Excellence, with an interdisciplinary internal research grant (IG 07/2022). M.L.M. acknowledges the Alexander von Humboldt Foundation for the Georg Forster postdoctoral scholarship. K.F.G. acknowledges Aminat Mohamed and Yitayal A. Workie for their expert comments during his experimental works. The authors acknowledge Franka Jahn from Leibniz-IPHT for SEM analysis and the European Fund Regional Development (EFRE) for partially funding EDX and XRD equipment under Project No. FKZ 2023 HSB 0025. The authors also acknowledge Tomáš Lednický for arranging the XPS measurement at the CzechNano Lab by MEYS CR (LM2023051) and funding from the European Union's Horizon Europe research and innovation program (grant agreement No 101109232).

REFERENCES

- (1) Chen, L.; De Borba, B.; Rohrer, J. *Determination Of Total And Free Sulfite In Foods And Beverages (Application Note, AN70379-EN 08/16S)*, 2016. <https://tools.thermofisher.com/content/sfs/brochures/AN-54-IEX-Sulfite-Food-Beverage-AN70379-EN.pdf>. (accessed 13 January 2025).
- (2) Koch, M.; Koppen, R.; Siegel, D.; Witt, A.; Nehls, I. Determination of total sulfite in wine by ion chromatography after in-sample oxidation. *J. Agric. Food Chem.* **2010**, *58* (17), 9463–9467.
- (3) *New EU Rules For 'Organic Wine' Agreed*. https://ec.europa.eu/commission/presscorner/detail/en/ip_12_113. (accessed 10 October 2024).
- (4) Kim, H. J. Determination of sulfite in foods and beverages by ion exclusion chromatography with electrochemical detection: Collaborative study. *J. AOAC Int.* **1990**, *73* (2), 216–222.
- (5) Espinosa, M.; Lanciki, A. A Simplified Method to Determine Total Sulphite Content in Food and Beverages via Ion Chromatography. *Column* **2020**, *16* (2), 12–16.
- (6) Mustafa, Y. F.; Chehardoli, G.; Habibzadeh, S.; Arzehgar, Z. Electrochemical detection of sulfite in food samples. *J. Electrochem. Sci. Eng.* **2022**, *12* (6), 1061–1079.
- (7) Pandi, K.; Sivakumar, M.; Chen, S.-M.; Sakthivel, M.; Raghavi, G.; Chen, T.-W.; Liu, Y.-C.; Madhu, R. Electrochemical Synthesis of Lutetium (III) Hexacyanoferrate/poly(aurine) Modified Glassy Carbon Electrode for the Sensitive Detection of Sulfite in Tap Water. *J. Electrochem. Soc.* **2018**, *165* (10), B469–B474.
- (8) Theisen, S.; Hansch, R.; Kothe, L.; Leist, U.; Galensa, R. A fast and sensitive HPLC method for sulfite analysis in food based on a plant sulfite oxidase biosensor. *Biosens. Bioelectron.* **2010**, *26* (1), 175–181.
- (9) Yilmaz, D.; Miranda, B.; Lonardo, E.; Rea, I.; De Stefano, L.; De Luca, A. C. SERS-based pH-Dependent detection of sulfites in wine by hydrogel nanocomposites. *Biosens. Bioelectron.* **2024**, *245*, 115836.
- (10) Nunes, G. S.; Toscano, I. A.; Barceló, D. Analysis of pesticides in food and environmental samples by enzyme-linked immunosorbent assays. *TrAC, Trends Anal. Chem.* **1998**, *17* (2), 79–87.
- (11) López Dávila, E.; Houbraken, M.; Gil Uday, Z.; Romero Romero, O.; Du Laing, G.; Spanoghe, P. ELISA, a feasible technique to monitor organophosphate, carbamate, and pyrethroid residues in local vegetables. Cuban case study. *SN Appl. Sci.* **2020**, *2* (9), 1487.
- (12) Iyer, P. V.; Ananthanarayan, L. Enzyme stability and stabilization—Aqueous and non-aqueous environment. *Process Biochem.* **2008**, *43* (10), 1019–1032.
- (13) Edberg, U.; Anttonen, M.-L.; Berg-Nilsen, K.; Blomberg, K.; Gjerstad, K. O.; Gustavsson, T.; Joner, P.; Loimaranta, J.; Mustranta, A.; Oksanen, M.; et al. Enzymatic determination of sulfite in foods: NMKL interlaboratory study. *J. AOAC Int.* **1993**, *76* (1), 53–58.
- (14) Huang, Y.; Ren, J.; Qu, X. Nanozymes: Classification, Catalytic Mechanisms, Activity Regulation, and Applications. *Chem. Rev.* **2019**, *119* (6), 4357–4412.
- (15) Lyu, Y.; Scrimin, P. Mimicking Enzymes: The quest for powerful catalysts from simple molecules to nanozymes. *ACS Catal.* **2021**, *11* (18), 11501–11509.
- (16) Li, S.; Zhang, Y.; Wang, Q.; Lin, A.; Wei, H. Nanozyme-Enabled Analytical Chemistry. *Anal. Chem.* **2022**, *94* (1), 312–323.
- (17) Lei, L.; Yang, X.; Song, Y.; Huang, H.; Li, Y. Current research progress on laccase-like nanomaterials. *New J. Chem.* **2022**, *46* (8), 3541–3550.
- (18) Liang, M.; Yan, X. Nanozymes: From New Concepts, Mechanisms, and Standards to Applications. *Acc. Chem. Res.* **2019**, *52* (8), 2190–2200.
- (19) Mekonnen, M. L.; Abda, E. M.; Csáki, A.; Fritzsche, W. Frontiers in Laccase Nanozymes-Enabled Colorimetric Sensing: A review. *Anal. Chim. Acta* **2025**, *1337*, 343333.
- (20) Achamyeleh, A. A.; Ankala, B. A.; Workie, Y. A.; Mekonnen, M. L.; Abda, E. M. Bacterial Nanocellulose/Copper as a Robust Laccase-Mimicking Bionanozyme for Catalytic Oxidation of Phenolic Pollutants. *ACS Omega* **2023**, *8* (45), 43178–43187.
- (21) Mekonnen, E. G.; Shitaw, K. N.; Hwang, B.-J.; Workie, Y. A.; Abda, E. M.; Mekonnen, M. L. Copper nanoparticles embedded fungal chitosan as a rational and sustainable bionanozyme with robust laccase activity for catalytic oxidation of phenolic pollutants. *RSC Adv.* **2023**, *13* (46), 32126–32136.
- (22) Xu, X.; Wang, J.; Huang, R.; Qi, W.; Su, R.; He, Z. Preparation of laccase mimicking nanozymes and their catalytic oxidation of phenolic pollutants. *Catal. Sci. Technol.* **2021**, *11* (10), 3402–3410.
- (23) Zhang, M.; Zhang, Y.; Yang, C.; Ma, C.; Tang, J. A smartphone-assisted portable biosensor using laccase-mineral hybrid microflowers for colorimetric determination of epinephrine. *Talanta* **2021**, *224*, 121840.
- (24) Yang, L.; Guo, X.-Y.; Zheng, Q.-H.; Zhang, Y.; Yao, L.; Xu, Q.-X.; Chen, J.-C.; He, S.-B.; Chen, W. Construction of platinum nanozyme by using carboxymethylcellulose with improved laccase-like activity for phenolic compounds detection. *Sens. Actuators, B* **2023**, *393*, 134165.
- (25) Qin, W.; Su, L.; Yang, C.; Ma, Y.; Zhang, H.; Chen, X. Colorimetric Detection of Sulfite in Foods by a TMB–O₂–Co₃O₄ Nanoparticles Detection System. *J. Agric. Food Chem.* **2014**, *62* (25), 5827–5834.
- (26) Huang, H.; Li, M.; Hao, M.; Yu, L. L.; Li, Y. A novel selective detection method for sulfide in food systems based on the GMP-Cu nanozyme with laccase activity. *Talanta* **2021**, *235*, 122775.
- (27) Yin, Q.; Wang, Y.; Wang, D.; Yang, Y.; Zhu, Y. A colorimetric detection of dopamine in urine and serum based on the CeO₂@ZIF-8/Cu-CDs laccase-like nanozyme activity. *Luminescence* **2024**, *39* (2), No. e4684.
- (28) Le, T. N.; Le, X. A.; Tran, T. D.; Lee, K. J.; Kim, M. I. Laccase-mimicking Mn–Cu hybrid nanoflowers for paper-based visual detection of phenolic neurotransmitters and rapid degradation of dyes. *J. Nanobiotechnol.* **2022**, *20* (1), 358.
- (29) Tang, Q.; Zhou, C.; Shi, L.; Zhu, X.; Liu, W.; Li, B.; Jin, Y. Multifunctional Manganese-Nucleotide Laccase-Mimicking Nanozyme for Degradation of Organic Pollutants and Visual Assay of Epinephrine via Smartphone. *Anal. Chem.* **2024**, *96* (11), 4736–4744.
- (30) Wang, Q.; Wang, X.; Wei, H. Spinel-Oxide-Based Laccase Mimics for the Identification and Differentiation of Phenolic Pollutants. *Anal. Chem.* **2022**, *94* (28), 10198–10205.
- (31) Liang, S.; Wu, X.-L.; Xiong, J.; Yuan, X.; Liu, S.-L.; Zong, M.-H.; Lou, W.-Y. Multivalent Ce-MOFs as biomimetic laccase nanozyme for environmental remediation. *Chem. Eng. J.* **2022**, *450*, 138220.
- (32) Wang, P.; Chen, R.; Jia, Y.; Xu, Y.; Bai, S.; Li, H.; Li, J. Cu-chelated polydopamine nanozymes with laccase-like activity for

photothermal catalytic degradation of dyes. *J. Colloid Interface Sci.* **2024**, *669*, 712–722.

(33) Chen, Z.; Yu, Y.; Gao, Y.; Zhu, Z. Rational Design Strategies for Nanozymes. *ACS Nano* **2023**, *17* (14), 13062–13080.

(34) Geleto, S. A.; Gutema, B. T.; Ariti, A. M.; Ankala, B. A.; Achamyeleh, A. A.; Mekonnen, E. G.; Mekonnen, K. N.; Workie, Y. A.; Abda, E. M.; Mekonnen, M. L. 2 - Classification of nanozymes. In *Nanozymes*, Tripathi, R. M.; Pudake, R. N.; Huang, P.; Horzum, N., Eds.; Elsevier, 2024, pp 19–44.

(35) Saberi, D.; Mansourinejad, S.; Shadi, A.; Habibi, H. One-pot synthesis of a highly disperse core–shell CuO–alginate nanocomposite and the investigation of its antibacterial and catalytic properties. *New J. Chem.* **2021**, *46* (1), 199–211.

(36) Srinivasan, B. A guide to the Michaelis-Menten equation: Steady state and beyond. *FEBS J.* **2022**, *289* (20), 6086–6098.

(37) European Medicines Agency. *ICH Q2(R2) Validation of analytical procedures - Scientific guideline*. European Medicines Agency, 2023.

(38) Rui Rodrigues, J.; Lagoa, R. Copper Ions Binding in Cu-Alginate Gelation. *J. Carbohydr. Chem.* **2006**, *25* (2–3), 219–232.

(39) Wang, Z.; Mi, B. Environmental Applications of 2D Molybdenum Disulfide (MoS₂) Nanosheets. *Environ. Sci. Technol.* **2017**, *51* (15), 8229–8244.

(40) Wu, Y.; Yuan, L.; Sheng, N.-A.; Gu, Z.-Q.; Feng, W.-H.; Yin, H.-Y.; Morsi, Y.; Mo, X.-M. A soft tissue adhesive based on aldehyde-sodium alginate and amino-carboxymethyl chitosan preparation through the Schiff reaction. *Front. Mater. Sci.* **2017**, *11*, 215–222.

(41) Mahl, C. R. A.; Bataglioli, R. A.; Calais, G. B.; Taketa, T. B.; Beppu, M. M. Role of Alginate Composition on Copper Ion Uptake in the Presence of Histidine or Beta-Amyloid. *Molecules* **2022**, *27* (23), 8334.

(42) Chai, T.-Q.; Wang, J.-L.; Chen, G.-Y.; Chen, L.-X.; Yang, F.-Q. Tris-Copper Nanozyme as a Novel Laccase Mimic for the Detection and Degradation of Phenolic Compounds. *Sensors* **2023**, *23* (19), 8137.

(43) Lei, Y.; He, B.; Huang, S.; Chen, X.; Sun, J. Facile Fabrication of 1-Methylimidazole/Cu Nanozyme with Enhanced Laccase Activity for Fast Degradation and Sensitive Detection of Phenol Compounds. *Molecules* **2022**, *27* (15), 4712.

(44) Gao, L.; Zhuang, J.; Nie, L.; Zhang, J.; Zhang, Y.; Gu, N.; Wang, T.; Feng, J.; Yang, D.; Perrett, S.; Yan, X. Intrinsic peroxidase-like activity of ferromagnetic nanoparticles. *Nat. Nanotechnol.* **2007**, *2* (9), 577–583.

(45) Ariti, A. M.; Geleto, S. A.; Gutema, B. T.; Mekonnen, E. G.; Workie, Y. A.; Abda, E. M.; Mekonnen, M. L. Magnetite chitosan hydrogel nanozyme with intrinsic peroxidase activity for smartphone-assisted colorimetric sensing of thiabendazole. *Sens. Bio-Sens. Res.* **2023**, *42*, 100595.

(46) Nguyen, P. T.; Vu, T. H.; Kim, M. I. Histidine–cysteine–copper hybrid nanoflowers as active site-inspired laccase mimics for the colorimetric detection of phenolic compounds in PDMS microfluidic devices. *Sens. Actuators, B* **2024**, *413*, 135845.

(47) Afreen, S.; Shamsi, T. N.; Baig, M. A.; Ahmad, N.; Fatima, S.; Qureshi, M. I.; Hassan, M. I.; Fatma, T. A novel multicopper oxidase (laccase) from cyanobacteria: Purification, characterization with potential in the decolorization of anthraquinonic dye. *PLoS One* **2017**, *12* (4), No. e0175144.

(48) Tian, S.; Zhang, C.; Yu, M.; Li, Y.; Fan, L.; Li, X. Buffer species-dependent catalytic activity of Cu-Adenine as a laccase mimic for constructing sensor array to identify multiple phenols. *Anal. Chim. Acta* **2022**, *1204*, 339725.

(49) Wang, Y.; He, C.; Li, W.; Zhang, J.; Fu, Y. Catalytic performance of oligonucleotide-templated Pt nanozyme evaluated by laccase substrates. *Catal. Lett.* **2017**, *147*, 2144–2152.

(50) Song, J.; Su, P.; Yang, Y.; Yang, Y. Efficient immobilization of enzymes onto magnetic nanoparticles by DNA strand displacement: A stable and high-performance biocatalyst. *New J. Chem.* **2017**, *41* (14), 6089–6097.

(51) Payal, A.; Krishnamoorthy, S.; Elumalai, A.; Moses, J.; Anandharamkrishnan, C. A review on recent developments and applications of nanozymes in food safety and quality analysis. *Food Anal. Methods* **2021**, *14*, 1537–1558.

(52) Lajin, B.; Goessler, W. Exploring the sulfur species in wine by HPLC-ICPMS/MS. *Anal. Chim. Acta* **2019**, *1092*, 1–8.

(53) Wang, L.; Xu, L. Cyclic Voltammetric Determination of Free and Total Sulfite in Muscle Foods Using an Acetylferrocene–Carbon Black–Poly(vinyl butyral) Modified Glassy Carbon Electrode. *J. Agric. Food Chem.* **2014**, *62* (42), 10248–10253.

(54) *Sulfites in Wine*. <https://www.rawwine.com/learn/what-are-sulfites-in-wine/>. (accessed 9 January 2025).

(55) Malcomson, T.; Repiscak, P.; Erhardt, S.; Paterson, M. J. Protocols for Understanding the Redox Behavior of Copper-Containing Systems. *ACS Omega* **2022**, *7* (49), 45057–45066.

(56) Shrivastava, S.; Deshpande, P.; Daharwal, S. Key aspects of analytical method development and validation. *J. Ravishankar Univ.* **2018**, *31* (1), 32–39.

(57) Araujo, P. Key aspects of analytical method validation and linearity evaluation. *J. Chromatogr. B: Biomed. Sci. Appl.* **2009**, *877* (23), 2224–2234.

(58) Pandi, K.; Sivakumar, M.; Chen, S.-M.; Sakthivel, M.; Raghavi, G.; Chen, T.-W.; Liu, Y.-C.; Madhu, R. Electrochemical synthesis of lutetium (III) hexacyanoferrate/poly (taurine) modified glassy carbon electrode for the sensitive detection of sulfite in tap water. *J. Electrochem. Soc.* **2018**, *165* (10), B469.

(59) Ma, X.; Liu, C.; Shan, Q.; Wei, G.; Wei, D.; Du, Y. A fluorescein-based probe with high selectivity and sensitivity for sulfite detection in aqueous solution. *Sens. Actuators, B* **2013**, *188*, 1196–1200.

(60) Liang, T.; Liu, S.; Shen, T.; Chen, X.; Li, X.; Yan, X.; Sun, X.; Tian, M.; Wu, C.; Sun, X.; Zhong, K.; Li, Y.; Liu, X.; Tang, L. Chromene-derived red-fluorescent probes for sulfite detection in food and living cells based on an integrated ICT&PET platform. *Sens. Actuators, B* **2024**, *413*, 135864.

(61) Venkatchalam, K.; Asaithambi, G.; Rajasekaran, D.; Periasamy, V. A novel ratiometric fluorescent probe for “naked-eye” detection of sulfite ion: Applications in detection of biological SO₃²⁻ ions in food and live cells. *Spectrochim. Acta, Part A* **2020**, *228*, 117788.

(62) Hassan, S. S. H.; Kamel, A.; Amr, A. E.-G. E.; Abd-Rabboh, H. S. M.; Al-Omar, M. A.; Elsayed, E. A. A new validated potentiometric method for sulfite assay in beverages using cobalt (II) phthalocyanine as a sensory recognition element. *Molecules* **2020**, *25* (13), 3076.

(63) Yang, X.; Zhang, X.; Huang, Y. Oxygen vacancies rich Co-Mo metal oxide microspheres as efficient oxidase mimetic for colorimetric detection of sulfite. *Microchem. J.* **2023**, *189*, 108562.

(64) Yue, X.; Fu, L.; Wu, C.; Xu, S.; Bai, Y. Rapid Trace Detection of Sulfite Residue in White Wine Using a Multichannel Colorimetric Nanozyme Sensor. *Foods* **2023**, *12* (19), 3581.

(65) Lu, W.; Shu, J.; Wang, Z.; Huang, N.; Song, W. The intrinsic oxidase-like activity of Ag₂O nanoparticles and its application for colorimetric detection of sulfite. *Mater. Lett.* **2015**, *154*, 33–36.